A fluorine-labeled methotrexate as a probe for monitoring tumor antifolate pharmacokinetics: Synthesis, *in vitro* cytotoxicity, and pilot *in vivo* ^{19}F magnetic resonance spectra

William M. Spees,[1] Guangli Yang,[2] Darren Veach,[2] Maria Belen Rubio,[2] Jason A. Koutcher,[1,3,4] and William Bornmann[2]

[1] Department of Medical Physics, [2] Organic Synthesis Core Facility, Departments of [3] Medicine and [4] Radiology, Memorial Sloan-Kettering Cancer Center, New York, NY

Abstract

The synthesis and characterization of 3′-fluoromethotrexate (FMTX), a novel fluorine-labeled analogue of methotrexate, are presented. Molecular modeling studies indicate that the fluorine atom causes only minimal changes in the structure/binding in the complex of the antifolate with thymidine synthetase and dihydrofolate reductase (DHFR). The *in vitro* cytotoxicity of this compound is shown to be equivalent to that of the parent antifolate compound. While the focus of this report is the synthetic technique of FMTX, it is also demonstrated that tumor accumulation of the labeled compound *in vivo* can be observed via ^{19}F magnetic resonance spectroscopy (MRS) in a human tumor xenograft model. (Mol Cancer Ther. 2003;2:933–939)

Introduction

Noninvasive *in vivo* monitoring of the tumor uptake and retention of anti-neoplastic agents in patients via magnetic resonance spectroscopy (MRS) is often of limited utility due to the low plasma concentrations of drug achievable without unacceptable patient toxicity (1). There are exceptions wherein previously published reports have demonstrated the *in vivo* MR detection of chemotherapeutic agents administered at high doses including ^{13}C-labeled temozolomide (2), iproplatin investigated via ^{1}H MRS with multiple quantum coherence transfer techniques (3), and the ^{31}P-containing agents ifosfamide and cyclophosphamide (4). However, achieving acceptable signal-to-noise ratio in monitoring pharmacokinetics is challenging. One case in which more robust sensitivity can be achieved is the *in vivo* monitoring of the uptake and metabolism of 5-fluorouracil (FU) via ^{19}F MRS (see, *e.g.*, Ref. 5). *In vivo* monitoring of pharmacokinetics of FU is possible due to the high plasma concentration of drug that is achieved clinically, the relatively high sensitivity of the ^{19}F nucleus (83% of that of ^{1}H) in the MRS experiment, and the absence of background ^{19}F signal from endogenous metabolites.

Another antineoplastic agent routinely administered at very high dosage, achieving plasma concentrations up to 1 mM, is methotrexate. However, this antifolate is not ^{19}F-labeled. Herein we report on the synthesis and characterization of a fluorine-labeled methotrexate, 3′-fluoromethotrexate (FMTX). The *in vitro* cytotoxicity of the labeled compound is compared with that of the parent compound [methotrexate (MTX)] against a methotrexate-sensitive human sarcoma cell line (HT-1080). These results are consistent with molecular modeling studies that indicate similar binding affinities of MTX and FMTX with the enzymes dihydrofolate reductase (DHFR) and thymidine synthetase. Although previous reports in the literature detail the synthesis of other ^{19}F-labeled antifolates (6, 7), herein we demonstrate the first *in vivo* observation of tumor uptake and retention of a fluorine-labeled antifolate monitored noninvasively via ^{19}F MR in a xenograft tumor model in mice.

Materials and Methods

Chemistry/Molecular Modeling

General. High-resolution ^{1}H nuclear magnetic resonance (NMR) and ^{13}C NMR spectra were recorded on a Bruker AMX-400 spectrometer using tetramethylsilane as the internal chemical shift reference standard. IR spectra were recorded on a Perkin-Elmer 1600 Series Fourier transform spectrometer. Low-resolution electron ionization (EI) mass spectra were obtained on a PE SCIEX API 100 LC/MS system. All reagents were obtained either from Sigma-Aldrich (St. Louis, MO) or from Lancaster (Windham, NH) and vacuum-dried under P_2O_5 overnight before use. All solvents were reagent grade and distilled before use. Silica gel used for chromatography, MN-Kieselgel 60, was purchased from EM Science (Gibbstown, NJ). All reactions were carried out under argon using glassware dried in an oven at 80°C overnight and cooled under vacuum. The reaction mixtures were mechanically stirred using a magnetic stirring bar and stirring plate. Melting points were determined using a Mel-Temp II melting point apparatus fitted with a digital Barnart 115 thermocouple thermometer, and were uncorrected. Optical rotations were

Received 3/14/03; revised 6/11/03; accepted 7/8/03.

The costs of publication of this article were defrayed in part by the payment of page charges. This article must therefore be hereby marked advertisement in accordance with 18 U.S.C. Section 1734 solely to indicate this fact.

Grant support: NIH (R24CA83084, P50CA86438).

Requests for Reprints: Jason A. Koutcher, Department of Medical Physics/MRI, Memorial Sloan-Kettering Cancer Center, 1275 York Avenue, New York, NY 10021. Fax: (212) 717-3676. E-mail: koutchej@mskcc.org

recorded on a Fasco DIP-370 digital polarimeter with a sodium lamp at ambient temperature and recorded as $[\alpha]_D^{20}$ (c = g/100 ml). Molecular modeling and graphics renderings were performed using the SYBYL 6.8 (Tripos Associates Inc., St. Louis, MO) software package on a Silicon Graphics Octane2 R12000 workstation.

Synthesis of FMTX. Synthesis of FMTX was achieved via two alternative synthetic schemes (Schemes A and B) wherein the reaction product **6** is common to both methods as detailed in Figs. 1 and 2.

Di-*tert*-Butyl *N*-(3-Fluoro-4-Nitrobenzoyl)-L-Glutamate 3. A stirred slurry of 3-fluoro-4-nitrobenzoic acid **2** (1 g, 5.4 mmol, 1 eq) in dry toluene (20 ml) was treated with thionyl chloride (0.6 ml, 8.10 mmol, 1.5 eq) and the mixture was heated under reflux for 2 h. The solution was cooled to room temperature (RT) and the solvent and excess thionyl chloride were evaporated under vacuum. A solution of the resulting acid chloride in 20 ml of CH_2Cl_2 was added dropwise to a stirred mixture of di-*t*-butyl L-glutamate hydrochloride (1.6 g, 5.4 mmol, 1 eq) and Et_3N (1.5 ml, 10.8 mmol, 2 eq) in 20 ml of CH_2Cl_2 at 0°C (6). The reaction mixture was allowed to warm to RT and then stirred for 2 h. The solution was washed with water, dried over Na_2SO_4, and evaporated under vacuum. The crude product was purified by column chromatography on silica gel (Hex:EtOAc, 5:1 to 4:1) to give 1.6 g (69% yield) of product **3** as a yellow syrup. ^{1}H NMR ($CDCl_3$), δ 8.12 (t, 1H, J = 8.3 Hz), 7.80 (d, 1H, J = 11.1 Hz), 7.74 (d, 1H, J = 8.7 Hz), 7.58 (d, 1H, J = 6.6 Hz, NH), 4.62 (m, 1H), 2.44–2.34 (m, 2H), 2.20 (m, 1H), 2.09 (m, 1H), 1.50 (s, 9H), 1.44 (s, 9H); ^{13}C NMR ($CDCl_3$), δ 173.1, 170.6, 163.5 (d, J =1.3 Hz), 156.5, 153.9, 140.6 (d, J = 7.2 Hz), 138.8 (d, J = 7.8 Hz), 126.2 (d, J = 2.5 Hz), 122.9 (d, J = 4.2 Hz), 117.8, 117.5, 82.7, 81.3, 53.5, 31.5, 27.9, 27.9, 26.4; MS: $[M + H]^+$ 427.1, $[M + Na]^+$ 449.0, Calcd for $C_{20}H_{27}N_2O_7F$, 426.18.

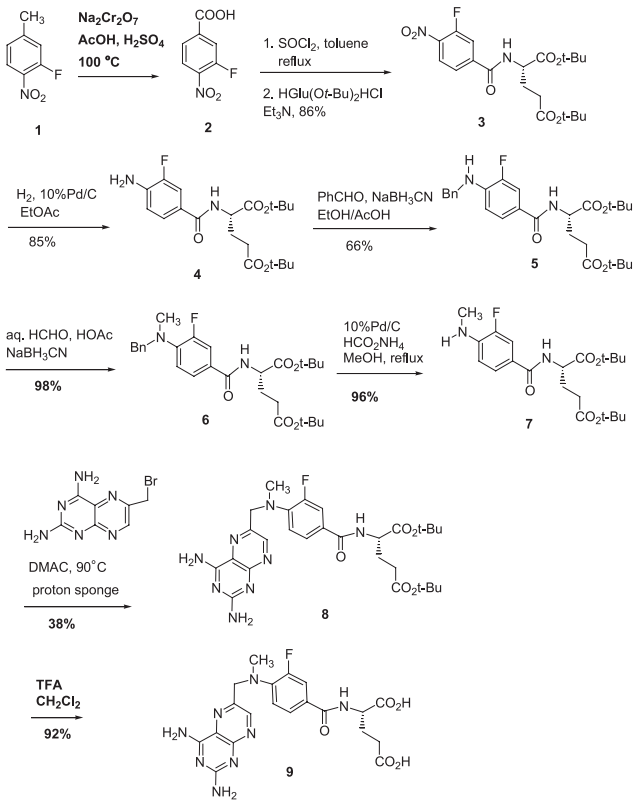

Figure1. Scheme A. Synthesis of FMTX.

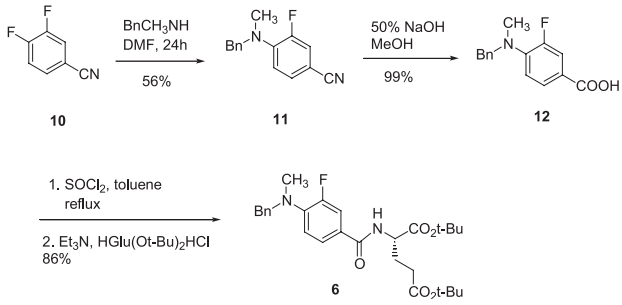

Figure 2. Scheme B. An alternate synthesis of intermediate 6.

Di-*tert*-Butyl *N*-(3-Fluoro-4-Aminobenzoyl)-L-Glutamate 4. A solution of the nitro compound **3** (1.54 g, 3.61 mmol, 1 eq) in 25 ml of EtOAc was stirred with 10% Pd-C (134 mg) under an atmosphere of H_2 until complete reaction was indicated by TLC (1 h). The reaction mixture was filtered through Celite and evaporated under vacuum. The crude mixture was purified by column chromatography of silica (Hex:EtOAc, 2:1) to give the amino compound **4** (1.18 g, 85% yield) as a white crystal. Mp 83–84°C; ^{1}H NMR (d_6-DMSO), δ 8.23 (d, 1H, J = 7.6 Hz), 7.59 (dd, 1H, J = 1.8, 12.8 Hz), 7.52 (d, 1H, J = 1.8, 8.3 Hz), 6.78 (t, 1H, J = 8.7 Hz), 4.34 (m, 1H), 2.33 (t, 2H, J = 7.5 Hz), 2.13 (br s, 2H, NH_2), 2.02 (m, 1H), 1.92 (m, 1H), 1.39 (s, 9H), 1.24 (s, 9H); ^{13}C NMR (d_6-DMSO), δ 171.5, 171.3, 150.5, 148.1, 139.8, 139.7, 124.6, 120.8 (d, J = 5.3 Hz), 114.5 (d, J = 4.7 Hz), 114.2, 114.0, 80.2, 79.6, 52.3, 31.3, 27.6, 27.5, 25.9; MS: $[M + H]^+$ 397.0, $[M + Na]^+$ 419.0, Calcd for $C_{20}H_{29}N_2O_5F$, 396.21.

Di-*tert*-Butyl *N*-(3-Fluoro-4-Benzylaminobenzoyl)-L-Glutamate 5. Sodium cyanoborohydride (1.67 g, 26.54 mmol, 2.4 eq) was added in small portions to a stirred solution of **4** (4.39 g, 11.06 mmol, 1 eq) benzaldehyde (1.6 ml, 15.49 mmol, 1.4 eq) and bromocresol green (~1 mg) in 50 ml of ethanol. After complete addition, acetic acid was added dropwise to adjust the solution to slightly acidic pH as determined by the indicator. The reaction solution was stirred for 24 h at RT, and during this time, acetic acid was added dropwise as necessary to maintain a slightly acidic solution. The acidic solution was extracted with EtOAc/Et_2O (1:1, v/v). The organic phase was washed with 10% NaOH, water, and saturated NaCl solution, dried over Na_2SO_4, and evaporated under vacuum to afford the crude product. Purification by column chromatography on silica gel (Hex:EtOAc, 3:1 to 1:1) gave the product **5** (3.54 g, 66%) as a white solid and recovered starting material **4** (909 mg, 21%). Mp 80–82°C; ^{1}H NMR ($CDCl_3$), δ 7.53 (dd, 1H, J = 2.0, 12.4 Hz), 7.45 (dd, 1H, J = 1.7, 8.4 Hz), 7.37 (m, 5 H),

6.78 (d, 1H, *J* = 7.3 Hz), 6.63 (t, 1H, *J* = 8.4 Hz), 4.63 (m, 1H), 4.42 (s, 2H), 2.39 (m, 1H), 2.32 (m, 1H), 2.20 (m, 1H), 2.02 (m, 1H), 1.59 (br s, 1H), 1.48 (s, 9H), 1.27 (s, 9H); ^{13}C NMR ($CDCl_3$), δ 172.6, 171.4, 165.9, 151.8, 149.4, 139.6, 139.5, 138.0, 128.8, 127.5, 127.3, 124.0, 121.9 (d, *J* = 5.7 Hz), 113.9, 113.6, 110.9 (d, *J* =3.5 Hz), 82.3, 80.8, 52.7, 47.3, 31.6, 28.0, 27.5; MS: $[M + H]^+$ 487.3, $[M + Na]^+$ 509.3, Calcd for $C_{27}H_{35}N_2O_5F$, 486.25.

Di-*tert*-Butyl *N*-(2-Fluoro-4-Benzylmethylaminobenzoyl)-L-Glutamate 6. Sodium cyanoborohydride (722 mg, 72.7 mmol, 1.5 eq) was added in small portions to a stirred solution of benzylamino compound **5** (3.54 g, 10.91 mmol, 1 eq) and formaldehyde (37% aqueous, 5.5 ml, 72.5 mmol, 10 eq) in 50 ml acetic acid at RT. The reaction solution was stirred for 1 h at RT. The acetic acid was evaporated under vacuum and the resulting residue was dissolved in EtOAc/Et_2O (1:1, v/v), washed with 1 N NaOH, water, and saturated NaCl solution, dried over Na_2SO_4, and evaporated under vacuum to afford the crude product. Purification by column chromatography on silica gel (Hex:EtOAc, 3:1) gave the product 6 (3.57 g, 98%).

Scheme B: An Alternate Three-Step Synthesis of Compound 6. Benzylmethylamine (1.5 ml, 11.85 mmol, 5 eq) was added dropwise to a solution of 3,4-difluorobenzonitrile **10** (330 mg, 2.37 mmol, 1 eq) in dry dimethylformamide (DMF) (5 ml) at 0°C. The reaction mixture was allowed to stir at RT overnight. The DMF was evaporated under vacuum and the residue chromatographed on silica gel (Hex:EtOAc, 9:1) to give 319 mg of pure product **11** (56%). This product was hydrolyzed with 50% of sodium hydroxide in methanol to reflux overnight. The reaction mixture was cooled to 0°C and concentrated HCl was added dropwise to pH = 2. The acidic solution was extracted with EtOAc. The organic phase was washed with saturated NaCl, dried over Na_2SO_4, and evaporated under vacuum to give 341 mg of the crude carboxylic acid **12** (99% yield). A stirred slurry of the carboxylic acid (341 mg, 1.31 mmol, 1 eq) in dry toluene (8 ml) was treated with thionyl chloride (144 μl, 1.97 mmol, 1.5 eq) and the mixture was heated under reflux for 2 h. The solution was cooled to RT and the solvent and excess thionyl chloride were evaporated under vacuum. A solution of the resulting acid chloride in 8 ml of CH_2Cl_2 was added dropwise to a stirred mixture of di-*t*-butyl L-glutamate hydrochloride (388 mg, 1.31 mmol, 1 eq) and Et_3N (0.4 ml, 2.62 mmol, 2 eq) in 8 ml of CH_2Cl_2 at 0°C. The reaction mixture was allowed to warm to RT and then stirred for 2 h. The solution was washed with water, dried over Na_2SO_4, and evaporated under vacuum. The crude product was purified by column chromatography on silica gel (Hex:EtOAc, 3:1) to give 633 mg (96% yield) of product **6** as a white solid. Mp = 71–72°C; IR (NaCl) 3346 (br m), 2978 (s), 2933 (m), 1730 (s), 1641 (s), 1616 (s), 1537 (m), 1509 (s), 1453 (m), 1368 (s), 1255 (s), 1153 cm^{-1} (vs); ^{1}H NMR ($CDCl_3$), δ 7.54 (dd, 1H, *J* = 2.1, 14.3 Hz), 7.48 (dd, 1H, *J* = 2.1, 8.4 Hz), 7.34–7.24 (m, 5H), 6.89 (d, 1H, *J* = 7.4 Hz), 6.81 (t, 1H, *J* = 8.7 Hz), 4.65 (dt, 1H, *J*t = 7.8 Hz, *J*d = 4.5 Hz), 4.44 (s, 2H), 2.86 (s, 3H), 2.43 (ddd, 1H, *J* = 6.9, 8.3, 16.6 Hz), 2.31 (ddd, 1H, *J* = 6.5, 7.9, 16.6 Hz), 2.26–2.17 (m, 1H), 2.08–1.98 (m, 1H), 1.49 (s, 9H), 1.42 (s, 9H); ^{13}C NMR ($CDCl_3$), δ 172.7, 172.3, 166.2 (d, *J* =1.3 Hz), 154.8, 152.4, 142.9 (d, *J* = 7.5 Hz), 138.3, 128.8, 128.1, 127.5, 127.4, 125.3 (d, *J* = 6.6 Hz), 123.9, 117.6 (d, *J* = 3.4 Hz), 116.1, 115.8, 82.5, 80.9, 58.7 (d, *J* = 6.8 Hz), 53.1, 39.2, 32.1, 28.4, 27.6; MS: $[M + H]^+$ 501.2, $[M + Na]^+$ 523.2, Calcd for $C_{28}H_{37}N_2O_5F$, 500.27; $[\alpha]_D^{20}$ +8.1 (*c* 1.13, $CHCl_3$).

Di-*tert*-Butyl *N*-(2-Fluoro-4-Methylaminobenzoyl)-L-Glutamate 7. Ammonium formate (1.12 g, 17.81 mmol, 5 eq) was added to a stirred suspension of benzylmethylamino compound **6** (3.57 g, 7.12 mmol, 1 eq) and 10% palladium on carbon (264 mg) in 50 ml of methanol at RT. The mixture was heated to reflux until TLC showed complete reaction. The reaction mixture was filtered through Celite and evaporated under vacuum. The crude mixture was purified by column chromatography of silica (Hex:EtOAc, 2:1) to give the amino compound **7** (2.82 g, 96% yield) as a white solid. Mp 95–96°C; IR (NaCl) 3377 (br), 2979, 2933, 1726, 1658, 1641, 1620, 1580, 1548, 1513, 1502, 1451, 1367, 1154 cm^{-1}; ^{1}H NMR ($CDCl_3$) δ 7.53–7.47 (m, 2H), 6.86 (d, 1H, *J* = 7.5 Hz), 6.62 (t, 1H, *J* = 8.5 Hz), 4.65 (m, 1H), 4.29 (br s, 1H, NH), 2.92 (d, 3H, *J* = 5.2 Hz), 2.43 (m, 1H), 2.31 (m, 1H), 2.22 (m, 1H), 2.03 (m, 1H), 1.49 (s, 9H), 1.42 (s, 9H); ^{13}C NMR ($CDCl_3$) δ 172.5, 171.5, 166.0 (d, *J* = 2.1 Hz), 151.6, 149.3, 140.7, 140.6, 123.9, 121.2 (d, *J* = 5.8 Hz), 113.3, 113.1, 109.8 (d, *J* = 3.7 Hz), 82.1, 80.6, 52.6, 31.6, 29.6, 27.9, 27.87, 27.40; MS: $[M + H]^+$ 411.1, $[M + Na]^+$ 433.1, Calcd for $C_{21}H_{31}N_2O_5F$, 410.22; $[\alpha]_D^{20}$ +10.5 (*c* 1.48, $CHCl_3$).

Di-*tert*-Butyl *N*-(2-Fluoro-4-Amino-4-Deoxy-N-Methyl-Pteroyl)-L-Glutamate 8. The amine **7** (887 mg, 2.16 mmol, 1 eq) was stirred with bromomethyldiaminopteridine [which was prepared according to the method of Piper and Montgomery (8) as modified by Boyle and Pfleiderer (9); 80% purity, 1.02 g, 2.46 mmol, 1.1 eq] in 6 ml of dry DMAC at 90°C for 1 h. ''Proton sponge'' (Aldrich Chemical Co., Milwaukee, WI; 480 mg, 2.24 mmol, 1 eq) was then added and the reaction was continued for an additional hour. The solvent was removed under vacuum. The dark residue was treated with 50 ml of $CHCl_3$ containing 1 ml of Et_3N and adsorbed in silica gel. Column chromatography on silica gel ($CHCl_3$:EtOH, 4:1) provided almost pure product. Another column chromatography was performed to obtain 477 mg of pure product **8** (38% yield) as a yellow solid. Mp 160–164°C; ^{1}H NMR (d_6-DMSO), δ 9.09 (br s), 8.65 (s, 1H), 8.40 (d, 1H, *J* = 7.5 Hz), 7.87 (br s), 7.67 (m, 2H), 7.56 (br s), 7.06 (t, 1H, *J* = 8.7 Hz), 6.82 (br s), 4.62 (s, 2H), 4.29 (m, 1H), 3.00 (s, 3H), 2.31 (t, 2H, *J* = 7.3 Hz), 2.03–1.87 (m, 2H), 1.39 (s, 9H), 1.37 (s, 9H); ^{13}C NMR (d_6-DMSO), δ 171.4, 171.1, 165.1 (d, *J* = 1.5 Hz), 162.7, 162.8, 155.0, 153.6, 151.2, 149.3, 145.5, 141.4, 141.3, 125.0 (d, *J* = 6.4 Hz), 124.3, 121.2, 117.6 (d, *J* = 3.6 Hz), 115.3, 115.1, 80.5, 76.7, 56.9 (d, *J* = 6.6 Hz), 52.4, 40.3, 31.3, 27.6, 27.6, 25.1; MS: $[M + H]^+$ 585.4, $[M + Na]^+$ 607.4, Calcd for $C_{28}H_{37}N_8O_5F$, 584.28.

***N*-(2-Fluoro-4-Amino-4-Deoxy-*N*-methyl-pteroyl)-L-Glutamic Acid 9.** The protected fluoromethotrexate **8** (750 mg, 1.28 mmol) was dissolved in 12 ml of CH_2Cl_2 and 6 ml

of trifluoroacetic acid (TFA) was added dropwise. After stirring for 2 h at RT, the reaction mixture was thoroughly evaporated under vacuum. The residue was dissolved in 0.01 N NaOH. The pH was the adjusted to 4.2–4.4 by addition of 1 N HCl giving a bright yellow precipitate. Filtration and washing with cold water provided the final product **9** (554 mg, 92% yield) as a bright yellow solid. Mp: 220–223C (decomp.); ^{1}H NMR (d_6-DMSO), δ 8.65 (s, 1H), 8.44 (d, 1H, J = 7.6 Hz), 7.76 (br s, 1H), 7.69 (m, 2H), 7.42 (br s, 1H), 7.06 (t, 1H, J = 8.8 Hz), 6.76 (br s, 2H), 4.62 (s, 2H), 4.36 (m, 1H), 3.00 (s, 3H), 2.32 (t, 2H, J = 7.5 Hz), 2.07 (m, 1H), 1.92 (m, 1H); ^{13}C NMR (d_6-DMSO), δ 173.9, 173.5, 165.1, 162.7, 162.5, 154.6, 153.7, 151.3, 145.9, 141.4, 141.4, 125.2, 125.2, 121.3, 117.7, 57.0, 51.9, 40.0, 30.5, 26.0; MS: $[M + H]^+$ 472.9, Calcd for $C_{20}H_{21}N_8O_5F$, 472.16; $[\alpha]_D^{20}$ +16.5 (c 0.87, 1 N NaOH).

Molecular Modeling. The Protein Data Bank (PDB) coordinate file for the thymidylate synthetase (TS)-methotrexate cocrystal structure was obtained from PDB (1AXW). The atom types for the inhibitor and cofactor dUMP were corrected, hydrogen atoms were added, and the protein C and N endgroups were fixed using the SYBYL/BIOPOLYMER module. Protein atomic charges were assigned with the Kollman all-atom charge set and inhibitor/cofactor charges were calculated using the Gasteiger-Hückel method. The complex was minimized using the Powell method, the Tripos Force Field, and 0.05 kcal/mol • Å rms gradient as the convergence criterion. All protein and cofactor heavy atoms (inherent to the crystal structure) were constrained in an aggregate during minimizations. Surfaces and cartoon diagrams were created within SYBYL using the MOLCAD surface dialog. Because we cannot directly compare the position of the ligand atoms in the X-ray structure with a minimized model, we required a minimized MTX:TS template. To create this model, the MTX:TS complex was minimized using the methods above. The conformation of MTX in the binding pocket changed only very slightly after minimization. MTX was replaced with FMTX and was again minimized as above.

An analogous study of the DHFR:MTX and FMTX complexes with NADPH was performed beginning with the X-ray structure of the MTX:DHFR complex of the *Mycobacterium tuberculosis* DHFR enzyme (10).

In Vitro Cytotoxicity

The cytotoxicity of FMTX was compared with that of the parent compound MTX against the MTX-sensitive human sarcoma cell line HT-1080 (ATCC, Rockville, MD). Cultured cells were maintained as monolayer cultures in RPMI 1640 culture medium supplemented with 10% FCS at 37°C under a humidified 5% CO_2 atmosphere. For cytotoxicity assays, monolayer cells were trypsinized and plated in six-well culture plates (10 cm^2 per well) at a density of 1000 cells/well. After a period of 48 h to allow for cell attachment and the establishment of cell proliferation, the medium was aspirated and replaced with fresh medium. During drug exposure, culture medium was either normal medium or thymidine-free medium to determine the effect of thymidine salvage (11, 12). Thymidine-free medium was prepared from normal medium via treatment with thymidine phosphorylase (Sigma, St. Louis, MO) for 60 min at 37°C followed by heat inactivation of the thymidine phosphorylase at 55°C and filtration (0.22 μm filter). MTX and FMTX stock solutions (10 mM) were prepared in isotonic saline with pH adjusted to 7.4. After a period of 24 h drug exposure, culture medium was aspirated and replaced with fresh normal medium. Cells were incubated for a further 72–96 h and cell viability was determined via the sodium 3′-[1-(phenylaminocarbonyl)-3,4-tetrazolium]-bis(4-methoxy-6-nitro) benzene sulfonic acid hydrate (XTT)/phenazine methosulfate (PMS) assay (13, 14). This spectrophotometric assay indicates the level of cellular biochemical redox activity in each culture well relative to control, untreated cells as a measure of cell viability. Cytotoxicity (repeated in triplicate) was evaluated from drug concentration response curves and is reported in terms of IC_{50}, the concentration of drug that reduces HT-1080 cell viability by 50%. Results for MTX and FMTX were compared via Student's t test.

In Vivo ^{19}F MR Spectra of FMTX

A pilot *in vivo* ^{19}F MR study was performed according to institutionally approved protocols for the safe and humane treatment of animals. A LNCaP (human prostate cancer) tumor xenograft in a nude mouse was used to determine *in vivo* MR visibility of FMTX. Tumor growth was initiated by the injection of 0.2 ml of a slurry of $\sim 10^5$ cells. The tumor cell slurry was inoculated s.c. into the left flank of 6-week-old male nude (athymic) mice.

The ^{19}F chemical shift of FMTX was first determined at high field (B_0 = 9.4 T). FMTX dissolved in blood plasma was placed in the outer compartment of a coaxial 5-mm NMR tube with the inner compartment (3 mm outer diameter) containing TFA in D_2O. The ^{19}FMTX resonance was observed at 46.4 ppm with respect to the TFA chemical shift reference.

FMTX was administered via i.v. bolus tail-vein injection at a dosage of 400 mg/kg, a dosage comparable to that used clinically in humans (15). The mouse was unanesthetized for ^{19}F MR experiments. The mice crawl into a 60-ml syringe barrel (with air holes) which is used as an animal holder with the tumor protruding through a hole into a home-built 2 turn ^{19}F MR surface coil. The inner diameter of the surface coil was 0.8 cm with tumor volume that offered maximum filling factor (200–350 mm^3). The *in vivo* ^{19}F MR study was performed at 188 MHz (B_0 = 4.7 T) in a wide-bore (33 cm diameter) small animal imaging system (GE Omega, Fremont, CA) with the tumor in a temperature control/susceptibility matching water bath (16). For the *in vivo* ^{19}F MR experiment (pulse and acquire), acquisition parameters included a 60° pulse-width with a pulse repetition time (T_R) of 2 s, 10,000 Hz sweep-width, 1024 complex data points per free induction decay (FID), and a summation of 256 FIDs per spectrum (9 min/spectrum). An external chemical shift reference standard of 100 mM TFA in D_2O was held in an 18-μl glass microsphere.

To optimize the acquisition parameters for future studies, the spin-lattice relaxation time T_1 was determined (17). An estimate of the *in vivo* FMTX T_1 value was made for a phantom sample of 7 mM FMTX dissolved in blood plasma at 37°C and 4.7 T with the inversion-recovery pulse sequence. The resonance intensity data of the 180°-τ-90°-acquire pulse sequence was fit, as shown in Fig. 3, to the equation:

$$M(\tau) = M_0 - C \cdot M_0 e^{-\tau/T_1} \qquad (A)$$

wherein the constant C allows for any error in the calibration of the 90° or 180° pulses. Resonance intensities were determined via modeling of the time-domain NMR signal data using the jMRUI software package run on a PC (18). From the fit to Eq. A, a T_1 value of 0.60 s was determined.

Results

Synthesis of FMTX

The synthetic route for FMTX was essentially the same as that of 3′-fluoroaminopterin (6). The synthesis was readily accomplished in eight steps starting from 3-fluoro-4-nitro-toluene **1** as outlined in Scheme A (Fig. 1). Thus, standard sodium dichromate oxidation of **1** afforded **2**, which was subsequently converted into the acid chloride by treatment with thionyl chloride in refluxing toluene. Addition of the isolated acid chloride to di-*tert*-butyl-L-glutamate hydrochloride in dichloromethane containing two equivalents of triethylamine at 0°C gave amide **3** in 69% yield. At this point, the hydrogenolysis of the nitro group to the corresponding amine was done at atmospheric pressure and RT to give *p*-aminobenzoyl moiety **4** in 85% yield. The resulting amine was transformed into the corresponding benzyl amine **5** by reductive amination with benzaldehyde using the standard sodium cyanoborohydride methodology. With the benzyl group in place, monomethylation of the benzyl amine was easily achieved via a subsequent second reductive amination with formaldehyde to give methylbenzyl amine **6** in 98% yield. Hydrogenolysis using 10% palladium on carbon with ammonium formate in refluxing methanol gave methyl amine **7** in 90% yield. Condensation with 6-(bromomethyl)-2,4-pteridinediamine hydrobromide (8, 9) in dimethylacetamide at 90°C with proton sponge gave the fully assembled di-*tert*-butyl-3′-fluoromethotrexate **8** in 38% yield after chromatography. Subsequent deprotection with TFA in dichloromethane gave FMTX **9** in 92% yield.

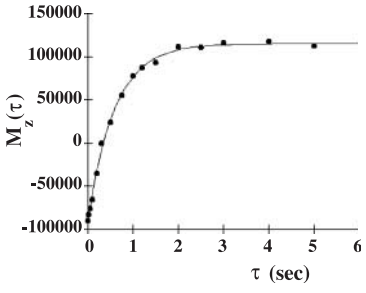

Figure 3. Inversion recovery data fit to Eq. A resulted in an estimated T_1 value of 0.60 s (r = 0.99) for FMTX in a blood plasma phantom sample at 4.7 T and 37°C.

An alternate synthesis of compound **6** (Fig. 2) was accomplished in four steps starting with 3,4-difluorobenzonitrile (Scheme B). Initial displacement of the fluorine at C-4 with methyl benzylamine in DMF at RT afforded compound **11** in 98% yield. Hydrolysis of the nitrile with 50% sodium hydroxide gave the resulting acid **12** in 98% isolated yield. This acid was then converted to the final compound **9** as previously described in 99% yield.

Molecular Modeling

The energy-minimized structures of the complexes of MTX and FMTX with the enzymes TS and DHFR demonstrate that the introduction of the fluorine label at the 3′ position of MTX results in only very small differences in the binding of the inhibitor in the antifolate-enzyme complexes. Fig. 4 shows the very small differences in the geometry of the inhibitors MTX and FMTX in these energy-minimized computer models. The modeling results also indicate only very slight differences in the binding energy between the MTX-enzyme and FMTX-enzyme complexes. The FMTX complexes appear to be slightly more favorable energetically, but not to a significant extent. Binding energies of the antifolate complexes with TS and DHFR differ by 1.4 and 3.7 kcal/mol, respectively. This suggests that FMTX may bind slightly better than MTX in both proteins.

In Vitro Cytotoxicity of MTX and FMTX

Table 1 and Fig. 5 display the cytotoxicity data for the two antifolates, MTX and FMTX, against the MTX-sensitive human sarcoma cancer HT-1080. The cytotoxicity of FMTX is slightly greater than that of the unlabeled MTX although these differences are not statistically significant ($P > 0.05$). These biological results are to be expected based on the similar binding energies of MTX and FMTX for the target enzymes DHFR and TS predicted by molecular modeling. It is also apparent that the presence of exogenous thymidine in the culture medium reduces cytotoxicity.

Pilot *in Vivo* ^{19}F MR Spectra of FMTX in LNCaP Xenograft Tumor

Fig. 6 demonstrates that tumor uptake of FMTX is readily detectable *in vivo* with good temporal resolution (9 min per spectrum). The surface coil MR experiment localizes ^{19}F signal to the sensitive volume of the coil (*i.e.*, the volume filled with tumor), thus it is assured that the signal intensity represents concentration of FMTX in the tumor. *In vivo*, the chemical shift of FMTX is in the range from 46.5 to 46.9 ppm with respect to the external reference solution of TFA. In this pilot study, we did not follow the full time course of FMTX tumor wash-in and washout as the goal was simply to demonstrate MR visibility of the compound *in vivo*. Also,

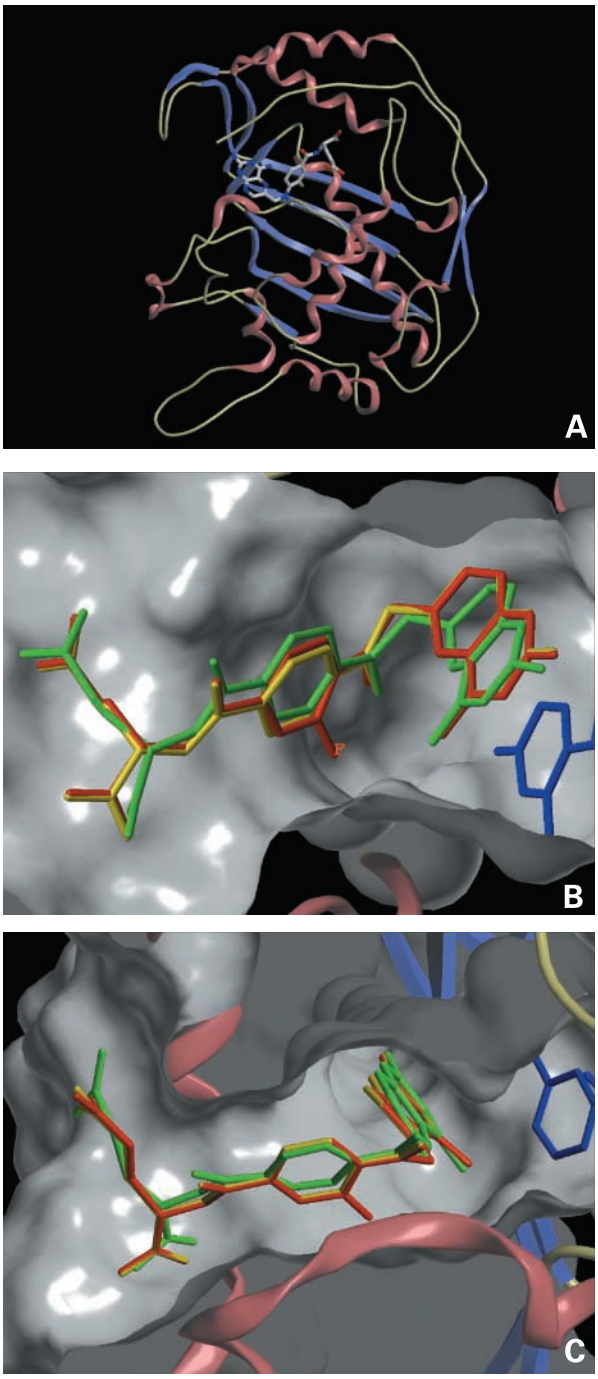

Figure 4. **A,** *top,* FMTX:TS energy minimized structure. **B,** *center,* thymidine synthetase-MTX and FMTX energy minimized complexes overlayed with the X-ray structure (MTX in *green*) of the complex. **C,** *bottom, M. tuberculosis* DHFR-MTX (MTX in *yellow*) and FMTX (*red*) energy minimized complexes overlayed with the X-ray structure (MTX in *green*) of the complex.

this set of spectra was acquired under conditions wherein longitudinal magnetization was essentially fully relaxed. Knowledge of the T_1 of FMTX in plasma (0.60 s, as determined here) provides a good first estimate of the *in vivo* T_1 value at 4.7 T.

Table 1. IC_{50} values for the antifolates MTX and FMTX in normal RPMI 1640 culture medium and in medium without exogenous thymidine

Drug/medium condition[a]	IC_{50} for 24 h drug exposure
FMTX/normal medium	345 ± 117 nM
MTX/normal medium	445 ± 148 nM
FMTX/treated medium	26 ± 5 nM
MTX/treated medium	69 ± 19 nM

[a]Normal, RPMI 1640 + 10% FCS; treated, thymidine-free RPMI 1640 + 10% FCS.

Discussion

The primary focus of this report is to detail the chemical synthesis of FMTX, demonstrate that it has biological activity (as determined by *in vitro* cytotoxicity studies) similar to that of MTX, and that the compound can be detected *in vivo* with ^{19}F MRS in a pilot study. Both molecular modeling and *in vitro* cytotoxicity indicate that the presence of the fluorine label in FMTX causes minimal modification of the activity of the parent compound, MTX.

As noted, there have been other reports in the literature of synthesis of fluorine-containing analogues of MTX (6, 7). However, in studies that compared cytotoxic efficacy of MTX with one of these fluorine-containing analogues (in which the fluorine substitution was on the γ-glutamyl moiety of MTX, see Ref. 7), the cytotoxicity of the fluorine-containing species was found to be some three orders of magnitude lower. It was determined that this was the result of impaired poly-glutamylation of the fluorine-substituted species.

In a cohort of HT-1080 tumor xenografts that were subsequently sacrificed (n = 4, not shown), FMTX accumulated in the tumor for time points up to 234 min postinjection and remained at elevated levels until the conclusion of the ^{19}F MR observation (270 min

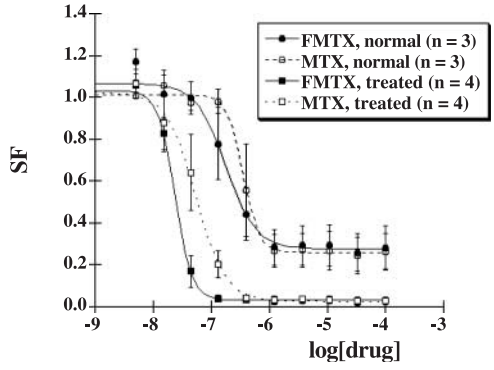

Figure 5. *In vitro* dose-response curves for the antifolates MTX and the 3′-fluoro-analogue, FMTX, against the human fibrosarcoma cell line HT-1080 for a 24-h exposure. Resulting IC_{50} values are reported in Table 1.

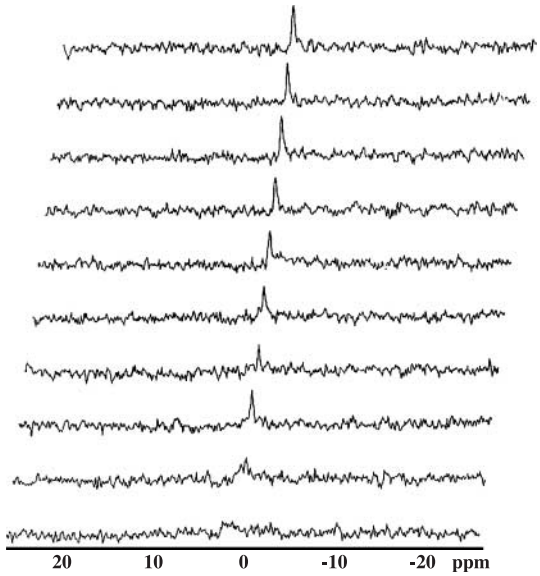

Figure 6. Serial, 9-min ^{19}F MR spectra showing the *in vivo* drug uptake of FMTX in a human LNCaP prostate tumor xenograft grown on the flank of a nude mouse. For display purposes, the raw FID data are multiplied by a 30-Hz exponential (matched filtering). MR acquisition parameters as described in ''Materials and Methods.''

postinjection). Quantitation of the FMTX resonance in this cohort indicated that the maximum mean intratumor FMTX tumor concentration was 0.73 ± 0.32 mM (mean ± SE) at 234 min postinjection.

Many of the clinically observed modes of resistance to MTX therapy involve reduced uptake and/or reduced intracellular retention (19, 20). We are currently investigating differences in pharmacokinetic parameters as observed by ^{19}F MR (maximum tumor concentration, rates of uptake, and washout) in a panel of MTX-sensitive and -resistant human sarcoma xenografts to determine the relationship between these pharmacokinetic parameters and therapeutic efficacy. The preliminary data (not shown herein) indicate that ^{19}F MR observation of tumor uptake/washout may be useful in assessing the likelihood of tumor response to therapy. Sensitive tumors appear to achieve significantly greater intratumoral concentration of FMTX than do MTX-resistant tumor xenografts (up to 3 times higher).

References

1. Rudin, M., Beckmann, N., Porszasz, R., Reese, T., Bochelen, D., and Sauter, A. *In vivo* magnetic resonance methods in pharmaceutical research: current status and perspectives. NMR Biomed., *12:* 69 – 97, 1999.

2. Artemov, D., Bhujwalla, Z. M., Maxwell, R. J., Griffiths, J. R., Judson, I. R., Leach, M. O., and Glickson, J. D. Pharmacokinetics of the ^{13}C labeled anticancer agent Temozolomide detected *in vivo* by selective cross-polarization transfer. Magn. Reson. Med., *34:* 338 – 342, 1995.

3. He, Q., Bhujwalla, Z. M., Maxwell, R. J., Griffiths, J. R., and Glickson, J. D. Proton NMR observation of the antineoplastic agent iproplatin *in vivo* by selective multiple quantum coherence transfer (Sel-MQC). Magn. Reson. Med., *33:* 414 – 416, 1995.

4. Payne, G. S., Pinkerton, C. R., Bouffet, E., and Leach, M. O. Initial measurements of ifosfamide and cyclophosphamide in patients using ^{31}P MRS: pulse-and-acquire, decoupling, and polarization transfer. Magn. Reson. Med., *44:* 180 – 184, 2000.

5. Wolf, W., Valuch, V., and Presant, C. A. Non-invasive ^{19}F-NMRS of 5-fluorouracil in pharmacokinetics and pharmacodynamic studies. NMR Biomed., *11:* 380 – 387, 1998.

6. Henkin, J. and Washtien, W. L. Novel fluorinated antifolates. Enzyme inhibition and cytotoxicity studies on 2′- and 3′-fluoroaminopterin. J. Med. Chem., *26:* 1193 – 1196, 1983.

7. Galivan, J., Inglese, J., McGuire, J. J., Nimec, Z., and Coward, J. K. γ-Fluoromethotrexate: synthesis and biological activity of a potent inhibitor of dihydrofolate reductase with greatly diminished ability to form poly-γ-glutamates. Proc. Natl. Acad. Sci. USA, *82:* 2598 – 2602, 1985.

8. Piper, J. R. and Montgomery, J. A. Preparation of 6-(bromomethyl)-2,4-pteridinediamine hydrobromide and its use in improved syntheses of methotrexate and related compounds. J. Org. Chem., *42:* 208 – 211, 1977.

9. Boyle, P. H. and Pfleiderer, W. Synthesis and reactivity of 2,4-diamino-6-(hydroxymethyl)-pteridins. Chem. Ber., *113:* 1514 – 1523, 1980.

10. Li, R., Sirawaraporn, R., Sirawaraporn, P. C. W., Wooden, J., Athappilly, F., Turley, S., and Hol, W. G. J. Three-dimensional structure of *M. tuberculosis* dihydrofolate reductase reveals opportunities for the design of novel tuberculosis drugs. J. Mol. Biol., *295:* 307 – 323, 2000.

11. Jackman, A. L., Taylor, G. A., Calvert, A. H., and Harrrap, K. R. Modulation of anti-metabolite effects: effects of thymidine on the efficacy of the quinazoline-based thymidylate synthetase inhibitor, CB3717. Biochem. Pharmacol., *33:* 3269 – 3275, 1984.

12. O'Dwyer, P. J., King, S. A., Hoth, D. F., and Leyland-Jones B. Role of thymidine in biochemical modulation: a review. Cancer Res., *47:* 3911 – 3919, 1987.

13. Lamontagne, P., Maion, G., and Page, M. Cytotoxicity testing using a soluble tetrazolium formazan derivative. Cell. Pharmacol., *1:* 171 – 174, 1994.

14. Scudiero, D. A., Shoemaker, R. H., Paull, K. D., Monks, A., Tierney, S., Nofziger, T. H., Currens, M. J., Seniff, D., and Boyd, M. R. Evaluation of a soluble tetrazolium/formazan assay for cell growth and drug sensitivity in culture using human and other tumor cell lines. Cancer Res., *48:* 4827 – 4833, 1988.

15. Roberts, D., Kidd, W., Pratt, C. B., Peck, C., and Grinnel, J. Serum levels of methotrexate by the ligand-binding assay after ''high-dose'' therapy for osteosarcoma. Cancer, *44:* 881 – 890, 1979.

16. Ballon, D., Mahmood, U., Jakubowski, A., and Koutcher, J. A. Resolution enhanced NMR spectroscopy in biological systems via magnetic susceptibility matched sample immersion chambers. Magn. Reson. Med., *30:* 754 – 758, 1993.

17. Becker, E. D., Ferretti, J. A., and Gambhir, P. N. Selection of optimum parameters for pulse Fourier transform nuclear magnetic resonance. Anal. Chem., *51:* 1413 – 1420, 1979.

18. Naressi, A., Couturier, C., Devos, J. M., Janssen, M., Mangeat, C., de Beer, R., and Graveron-Demilly, D. Java-based graphical user interface for the MRUI quantitation package. Magn. Reson. Mater. Phys. Biol. Med., *12:* 141 – 152, 2001.

19. Gorlick, R., Goker, E., Trippett, T., Waltham, M., Banerjee, D., and Bertino, J. R. Intrinsic and acquired resistance to methotrexate in acute leukemia. N. Engl. J. Med., *335:* 1041 – 1048, 1996.

20. Gorlick, R., Goker, E., Trippett, T., Steinheas, P., Elisseyeff, Y., Mazumdar, M., Flintoff, W. F., and Bertino, J. R. Defective transport is a common mechanism of acquired methotrexate resistance in acute lymphocytic leukemia and is associated with decreased reduced folate carrier expression. Blood, *89:* 1013 – 1018, 1997.